DOT/FAA/AR-10/37

Air Traffic Organization
NextGen & Operations Planning
Office of Research and
Technology Development
Washington, DC 20591

Evaluation of Low-Density Reticulated Foam to Mitigate Postcrash Fuel Fires

July 2011

Final Report

This document is available to the U.S. public through the National Technical Information Services (NTIS), Springfield, Virginia 22161.

This document is also available from the Federal Aviation Administration William J. Hughes Technical Center at actlibrary.tc.faa.gov.

U.S. Department of Transportation
Federal Aviation Administration

NOTICE

This document is disseminated under the sponsorship of the U.S. Department of Transportation in the interest of information exchange. The United States Government assumes no liability for the contents or use thereof. The United States Government does not endorse products or manufacturers. Trade or manufacturer's names appear herein solely because they are considered essential to the objective of this report. The findings and conclusions in this report are those of the author(s) and do not necessarily represent the views of the funding agency. This document does not constitute FAA policy. Consult the FAA sponsoring organization listed on the Technical Documentation page as to its use.

This report is available at the Federal Aviation Administration William J. Hughes Technical Center's Full-Text Technical Reports page: actlibrary.tc.faa.gov in Adobe Acrobat portable document format (PDF).

Technical Report Documentation Page

1. Report No. DOT/FAA/AR-10/37	2. Government Accession No.	3. Recipient's Catalog No.
4. Title and Subtitle EVALUATION OF LOW-DENSITY RETICULATED FOAM TO MITIGATE POSTCRASH FUEL FIRES		5. Report Date July 2011 6. Performing Organization Code
7. Author(s) Kevin L. Dowell, Sean Jankiewicz, and Leonard Lombardo		8. Performing Organization Report No.
9. Performing Organization Name and Address Department of the Army U.S. Army Aberdeen Test Center 400 Colleran Road Aberdeen Proving Ground, MD 21005-5059		10. Work Unit No. (TRAIS) 11. Contract or Grant No. DTC Project No. 2005-DT-ATC-FEDSP-D0158
12. Sponsoring Agency Name and Address U.S. Department of Transportation Federal Aviation Administration Air Traffic Organization NextGen & Operations Planning Office of Research and Technology Development Washington, DC 20591		13. Type of Report and Period Covered Final Report 14. Sponsoring Agency Code ANM-112

15. Supplementary Notes

The Federal Aviation Administration Airport and Aircraft Safety R&D Division COTR was Allan Abramowitz.

16. Abstract

Approximately 50% of the fatalities in survivable airplane crashes are due to postcrash fires. The objective of this study was to evaluate the performance of a new low-density (LD) reticulated polyurethane foam (LD foam) to mitigate postcrash airplane fires. Currently, reticulated foam is used in the fuel tanks of the C-130, A-10, and F-15 military aircraft for explosion protection. However, documentation on the use of reticulated foam to mitigate postcrash fires is limited and does not exist for the new LD foam. A series of sled tests were conducted to determine the effectiveness of LD foam to mitigate postcrash fuel-fed fires. LD foam was placed inside a simulated fuel tank and exposed to dynamic inertial forces experienced in a survivable airplane crash.

17. Key Words Aircraft accident, Low-density reticulated foam, Postcrash aircraft fire mitigation, Fireball	18. Distribution Statement This document is available to the U.S. public through the National Technical Information Service (NTIS), Springfield, Virginia 22161. This document is also available from the Federal Aviation Administration William J. Hughes Technical Center at actlibrary.tc.faa.gov.

19. Security Classif. (of this report) Unclassified	20. Security Classif. (of this page) Unclassified	21. No. of Pages 62	22. Price

Form DOT F 1700.7 (8-72) Reproduction of completed page authorized

ACKNOWLEDGEMENTS

The authors acknowledge the contributions of Christina McClung of Aberdeen Data Services Team (ADST) Logistics Engineering and Information Technology Company (Log.Sec/Tri-S).

TABLE OF CONTENTS

			Page
EXECUTIVE SUMMARY			xi
1.	INTRODUCTION		1
	1.1	Purpose	1
	1.2	Background	1
2.	TEST CONCEPT		1
3.	SYSTEM DESCRIPTION		3
4.	TESTS		12
	4.1	Phase I	12
		4.1.1 Objective	12
		4.1.2 Test Setup	12
		4.1.3 Results	13
		4.1.4 Technical Analysis	14
	4.2	Phase II	14
		4.2.1 Objectives	14
		4.2.2 Test Setup	15
		4.2.3 Test Results	15
		4.2.4 Technical Analysis	19
	4.3	Phase III	19
		4.3.1 Objectives	19
		4.3.2 Test Setup	19
		4.3.3 Test Results	20
		4.3.4 Technical Analysis	26
	4.4	Phase IV	27
		4.4.1 Objectives	27
		4.4.2 Test Setup	27
		4.4.3 Test Results	28
		4.4.4 Technical Analysis	30

4.5 Phase V 30

4.5.1 Objectives 30
4.5.2 Test Setup 30
4.5.3 Test Results 31
4.5.4 Technical Analysis 36

4.6 Phase VI 36

4.6.1 Objectives 36
4.6.2 Test Setup 37
4.6.3 Test Results 38
4.6.4 Technical Analysis 40

4.7 Phase VII 41

4.7.1 Objectives 41
4.7.2 Test Results 41

5. CONCLUSIONS 49

APPENDIX A—TEST SUMMARY

LIST OF FIGURES

Figure		Page
1	A 2-Foot Slice Taken From an Airplane Wing Fuel Tank	3
2	Simulated Fuel Tank and Components	4
3	Front View of Test Article	4
4	Rear View of Test Article	5
5	Extruded Aluminum Shoes Attached to the Bottom of the Fuel Tank	5
6	Test Rail	5
7	Braking System	7
8	Aluminum Brake Shroud	7
9	The PVC Pipe and Braking System	8
10	Pole Used to Activate Brakes and Rupture the Fuel Tank	8
11	Fuel Tank Rupture System Located on the Front of the Fuel Tank	9
12	Onboard DAS, Protective Compartment, and Wiring	10
13	High-Temperature-Resistant Insulation Covering the DAS and Wiring	10
14	Down-Range Photography Setup	11
15	Doppler Radar Head	11
16	Shot No. 1 Setup	12
17	Fuel Tank Leaving Rail	13
18	Shot No.1—Velocity vs Position	13
19	Shot No.1—Acceleration vs Position	14
20	Shot Nos. 2 and 3 Setup	15
21	Shot No. 2, Postrupture (dispersion of water)	16
22	Shot No. 2, Postrupture at Rest	16
23	Shot No. 3, Immediately After Rupture	17
24	Shot No. 3, Postrupture (dispersion of water)	17
25	Shot No. 3, Postrupture at Rest	17
26	Shot Nos. 2 and 3—Velocity vs Position	18
27	Shot Nos. 2 and 3—Acceleration vs Position	18
28	Shot No. 4 Pretest, Instrumented With Pressure Gauges	20
29	Shot No. 4, Postrupture (dispersion of water)	20
30	Shot No. 4, Postrupture at Rest	21
31	Shot No. 5, Fuel Tank With LD Foam—Notched Cutout for Pressure Gauges	21
32	Shot No. 5, Front View of the LD Foam in the Fuel Tank	22
33	Shot No. 5, Postrupture (dispersion of water)	22
34	Shot No. 6, Postrupture (dispersion of water)	22
35	Shot No. 6, Fuel Tank Filled With two Pieces of LD Foam	23
36	Shot No. 6, 3/4″ Deformation of LD Foam due to Inertia	23
37	Shot No. 7, Postrupture (dispersion of water)	24
38	Shot No. 7, Postrupture at Rest	24
39	Shot No. 8, Postrupture (dispersion of water)	25
40	Shot Nos. 4 to 8, Velocity vs Position	25
41	Shot Nos. 4 to 8, Acceleration vs Position	26
42	Shot No. 9, Protective Shroud Surrounding Braking System	28

43	Shot No. 9, Road Flares Added to Ignite Fuel	28
44	Shot No. 9, Velocity vs Position	29
45	Shot No. 9, Acceleration vs Position	29
46	Shot No. 10, Magnesium Flares Used to Ignite Fuel	31
47	Shot No. 10, Insulated Instrumentation Lines	31
48	Shot No. 10, Postrupture	32
49	Shot No. 10, Postrupture—Close-Up	32
50	Shot No. 10, Postrupture at Rest	33
51	Shot No. 11, Postrupture	33
52	Shot No. 11, Postrupture at Rest	34
53	Shot No. 11, Postrupture at Rest—Damaged Shroud	34
54	Shot No. 11, Velocity vs Position	35
55	Shot No. 11, Acceleration vs Position	35
56	Shot No. 11, Pressure Data	36
57	Shot No. 12, Fuel Tank Filled With two Pieces of LD Foam	37
58	Shot No. 12, Pretest	37
59	Shot No. 13, Fuel Tank Filled With two Pieces of LD Foam	38
60	Shot No. 12, Postrupture Fuel Test With LD Foam	38
61	Shot No. 12, Postrupture at Rest	39
62	Shot No. 13, Frontal View of LD Foam Removed From Fuel Tank	39
63	Shot Nos. 12 and 13, Velocity vs Position	40
64	Shot Nos. 12 and 13, Acceleration vs Position	40
65	Shot Nos. 4 and 5, Acceleration vs Position on Rail	42
66	Shot Nos. 4 and 5, Internal Pressures	43
67	Shot Nos. 4 and 5, Internal Pressures—Close-Up	43
68	Shot No. 4, Dispersion of Water While Decelerating (-1.25 g), no LD Foam	43
69	Shot No. 5, Dispersion of Water While Decelerating (-1.25 g), With LD Foam	44
70	Shot Nos. 11 and 13, Velocity vs Position	44
71	Shot Nos. 11 and 13, Acceleration vs Position	44
72	Shot Nos. 11 and 13, Comparison of Burning JP-8 Fireball	45
73	Shot No. 11 (no LD Foam), 1-Second Series of Tower Images of the Fireball	46
74	Shot No. 13 (LD Foam), 1-Second Series of Tower Images of the Fireball	47
75	Shot No. 11 (no LD Foam), 5-Second Series of Tower Images of the Fireball	48
76	Shot No. 13 (LD Foam), 5-Second Series of Tower Images of the Fireball	49

LIST OF TABLES

Table		Page
1	Test Phases	2
2	Test Matrix	2
3	Test Component Weights	6
4	Total Assembly Weight Based on Fill Level and Fuel Type	6

LIST OF ACRONYMS

CRDA	Cooperative Research and Development Agreement
DAS	Data acquisition system
FAA	Federal Aviation Administration
LD	Low density
PVC	Polyvinyl chloride

EXECUTIVE SUMMARY

Approximately 50% of the fatalities in survivable airplane crashes are due to postcrash fires. The objective of this study was to evaluate the performance of low-density (LD) reticulated polyurethane foam (LD foam) to mitigate airplane postcrash fires. The Aberdeen Test Center located in Aberdeen, MD, was tasked to design, fabricate, and execute a limited series of tests to determine the effectiveness of an LD foam insert designed to be placed inside a simulated fuel cell to reduce or stop the flow of fuel under dynamic inertial loading in a simulated crash.

The test article was a simulated fuel tank representing a section of a large commercial transport airplane. The interior dimensions of the fuel tank were 2′ wide, 7′ long, and 1′ high with a capacity of 104 gallons. The fuel tank was mounted to a sled filled with JP-8 fuel, or surrogate, and propelled down a test track at approximately 130 mph (190 ft/s). The fuel tank was ruptured by simulating a leading-edge impact resulting in a 5-inch opening in the front spar. Externally mounted magnesium flares on the fuel tank were used to ignite the leaking fuel. Brakes were simultaneously applied at the time of fuel tank rupture to decelerate and stop the sled. The sled was used to duplicate the dynamic forces experienced by an airplane during a crash.

The results showed that the LD foam (1.05 lb/ft^3, 40-45 pores/inch) reduced the initial fireball created at the fuel tank rupture and reduced the amount of fuel leakage from the fuel tank. Inspection of the LD foam-laden fuel tank at approximately 7 minutes after the fuel tank came to a stop showed that approximately 50% to 66% of the fuel remained in the fuel tank. Although the fuel continued to leak out of the fuel tank, it was at a very slow rate. The fuel tank without the LD foam was almost completely empty, with the exception of a small amount of fuel that remained at the bottom of the fuel tank.

1. INTRODUCTION.

1.1 PURPOSE.

Approximately 50% of the fatalities in survivable airplane crashes are due to postcrash fires. The objective of this study was to evaluate the performance of a new low-density (LD) reticulated polyurethane foam, hereinafter referred to as LD foam, to mitigate postcrash airplane fires. Currently, reticulated foam is used in the fuel tanks of the C-130, A-10, and F-15 military aircraft for explosion protection. However, documentation on the use of reticulated foam to mitigate postcrash fires is limited and does not exist for the new LD foam. A series of sled tests were conducted to determine the effectiveness of LD foam placed inside a simulated fuel tank, to mitigate postcrash fuel-fed fires when exposed to dynamic inertial forces experienced in a survivable airplane crash.

1.2 BACKGROUND.

Reticulated foam has been used for approximately 40 years to prevent fuel tank explosions caused by gunfire, electrical ignition, lightning strikes, and static charges. In addition, reticulated foam reduces fuel slosh during movement, thereby improving vehicle stability, control, and safety. Early reticulated foams showed limited product life and failed to control static charges in fuel tanks. However, these issues have been addressed in the current generation of the polyurethane-based reticulated foams. The use of reticulated foams for commercial and general aviation aircraft raises several concerns. These include the costs associated with the installation, required maintenance and inspection, and penalties regarding weight, displacement, and fuel retention. In addition to those listed above, the effectiveness of reticulated foams to reduce thermal injuries and fatalities associated with postcrash fires is in question.

The Federal Aviation Administration (FAA) was funded by Congress to evaluate the ability of a new, experimental LD foam (1.05 pcf, 40 to 45 pores per inch) to mitigate postcrash fires. Preliminary tests conducted under a Cooperative Research Development Agreement (CRDA) between Foamex International, Inc. (FOAMEX) and the FAA William J. Hughes Technical Center, Atlantic City International Airport, New Jersey, showed that the fuel misting and leakage through a simulated rupture could be mitigated using reticulated foam. However, additional tests were necessary to address the issues of fuel slosh, misting, and leakage when dynamic forces are present.

2. TEST CONCEPT.

The U.S. Army Aberdeen Test Center, located in Aberdeen, Maryland, in concert with the FAA, was contracted to design, fabricate, and conduct a series of simulated impact tests. The purpose was to determine the effectiveness of LD foam placed inside a simulated fuel tank to mitigate postcrash fuel-fed fires. The fuel tank would be exposed to dynamic inertial forces experienced in a survivable airplane crash. The tests were conducted on a simulated section of a large commercial transport airplane. Preliminary tests using water as a fuel surrogate were conducted to characterize the behavior of the test article. Water was used as an economic and environmental alternative to using JP-8 aviation jet fuel. The final four tests were conducted using JP-8 fuel with and without LD foam.

The simulated fuel tank was mounted to a sled and then filled with JP-8 fuel or water. The sled was propelled down a test track by a rocket-driven pusher sled at approximately 130 mph (190 fps) to duplicate the dynamic forces experienced by an airplane fuel tank during a crash. After rocket motor burnout and during the coast phase, the fuel tank was ruptured by simulating a leading-edge impact resulting in a 5-inch opening in the front spar of the wing fuel tank. A 5-inch opening was selected based on tests performed during the CRDA with FOAMEX. It was decided that a force resulting in a larger opening might lead to a catastrophic wing failure, which was beyond the scope of the project. Externally mounted magnesium flares on the fuel tank were used to ignite the leaking fuel. Brakes were simultaneously applied at the time of fuel tank rupture to decelerate and stop the sled in a slide out distance of approximately 500 ft. Since aircraft landing and takeoff velocities are comparable, a full fuel load was determined to represent a worst-case, postimpact fire scenario.

Seven test phases were conducted to evaluate the performance of the LD foam and are listed in table 1, and the corresponding test matrix is shown in table 2.

Table 1. Test Phases

Phase	Description
I	Demonstration
II	External braking system
III	Surrogate fuel performance evaluation
IV	Flare and water fill level evaluation
V	Fuel performance evaluation
VI	LD foam and fuel performance evaluation
VII	Comparative analysis of LD foam versus no LD foam

Table 2. Test Matrix

Phase	Shot No.	LD Foam	Fuel Type	Percent Full	Braked	Ruptured	Fire
I	1	No	Water	100	No	No	No
II	2	No	Water	100	Yes	Yes	No
	3	No	Water	100	Yes	Yes	No
III	4	No	Water	100	Yes	Yes	No
	5	Yes	Water	100	Yes	Yes	No
	6	Yes	Water	100	Yes	Yes	No
	7	No	Water	100	Yes	Yes	No
	8	No	Water	100	Yes	Yes	No
IV	9	No	Water	84	Yes	Yes	No
V	10	No	JP-8	100	Yes	Yes	Yes
	11	No	JP-8	100	Yes	Yes	Yes
VI	12	Yes	JP-8	100	Yes	Yes	Yes
	13	Yes	JP-8	100	Yes	Yes	Yes

The objective of this study was to determine the performance of LD foam during dynamic loading. Four areas of concern were:

- Recreate dynamic forces experienced during an airplane crash.
- Qualitatively assess fuel dispersion from ruptured fuel tank.
- Evaluate performance of LD foam to mitigate fireball and postcrash fuel fire.
- Evaluate performance of LD foam on the hydrodynamic ram effect (sloshing).

3. SYSTEM DESCRIPTION.

A simulated fuel tank was designed to represent a 2-foot slice of a commercial airplane's wing fuel tank (figure 1). To simplify the design and maximize aerodynamic braking, the fuel tank was designed as a box, and the impact angle was perpendicular to the front face of the fuel tank. The detailed dimensions of the test fuel tank are shown in figure 2. The limitations of the rail facility limited the fuel tank to be less than 2 ft wide. The fuel tank was ruptured by simulating a leading-edge impact resulting in a 5-inch circular opening in the front spar of the wing fuel tank. The opening was centered laterally on the front of the fuel tank (corresponding front spar) and centered 4.5 inches from the bottom of the fuel tank, which formed a 2-inch lip below the opening.

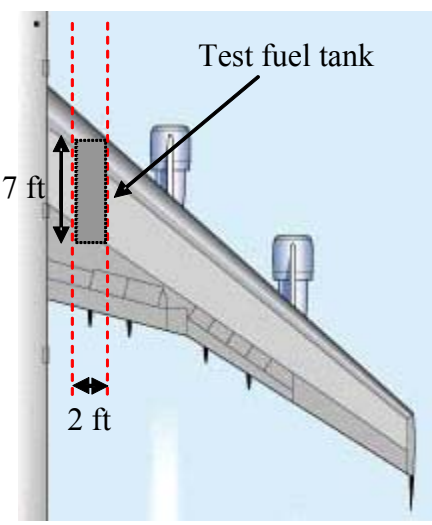

Figure 1. A 2-Foot Slice Taken From an Airplane Wing Fuel Tank

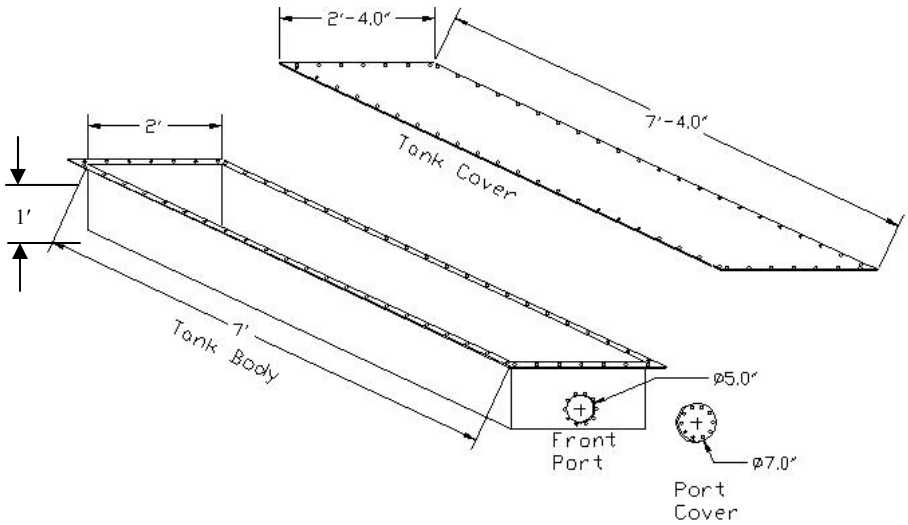

Figure 2. Simulated Fuel Tank and Components

The final test article included the following components: an aluminum fuel tank with brackets for flares, a Zuni rocket and pusher sled, three aluminum spacer plates, a fuel tank rupture system, and a brake assembly with a pressurized brake actuator (see figures 3 and 4). Rail guides made of extruded aluminum were welded to the bottom of the fuel tank, connecting the fuel tank to the rail. An illustration of the rail guide assembly attached to the bottom of the experimental fuel tank is shown in figure 5. The width of the rail was approximately 6 inches, and 2200 ft of the rail length were used for this test series. Figure 6 shows a section of the test rail.

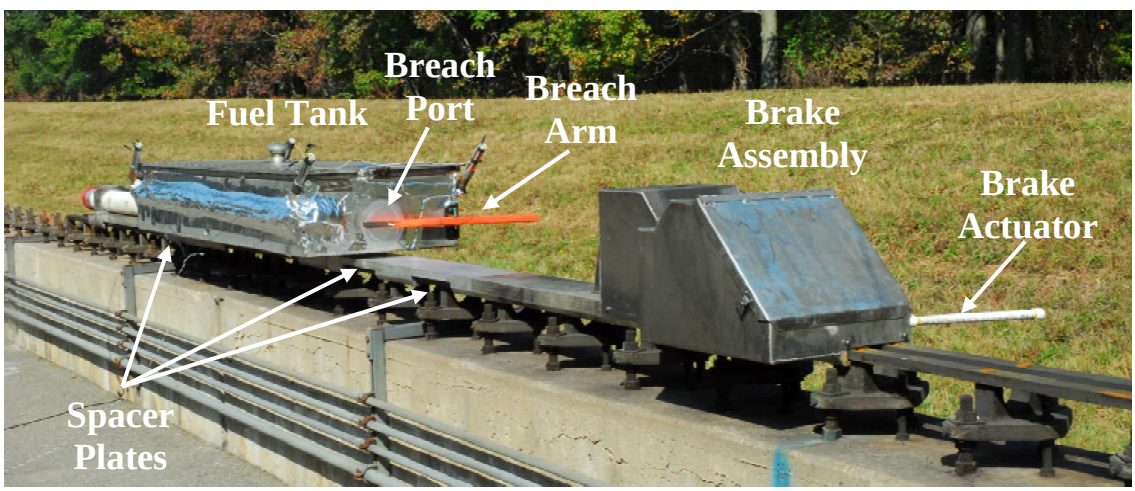

Figure 3. Front View of Test Article

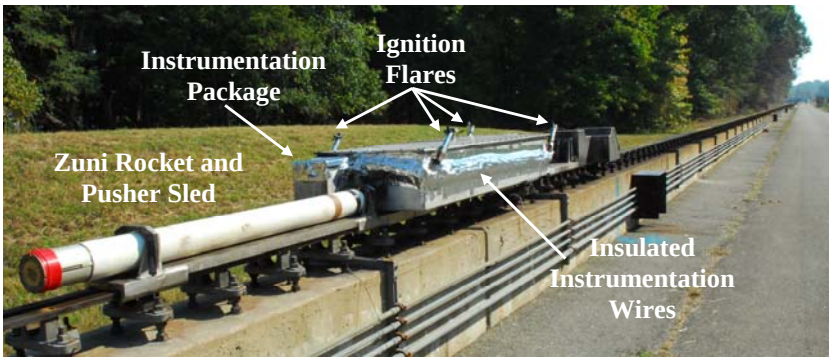

Figure 4. Rear View of Test Article

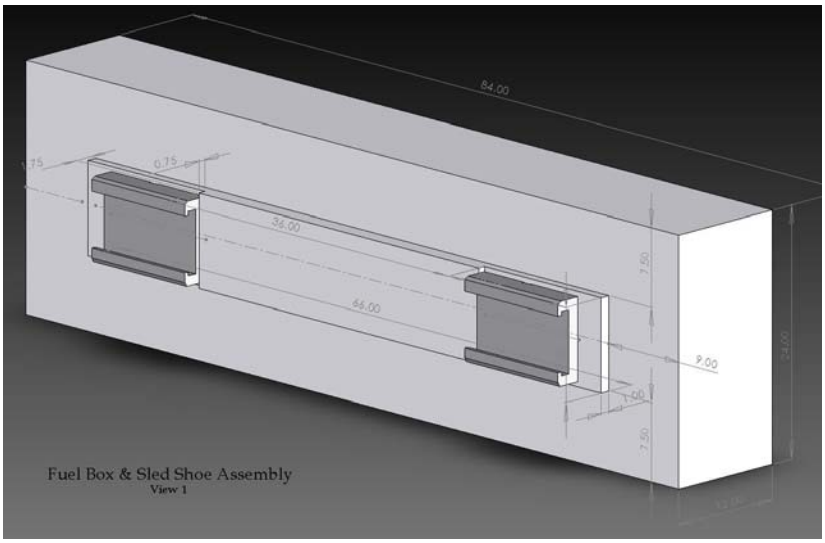

Figure 5. Extruded Aluminum Shoes Attached to the Bottom of the Fuel Tank

Figure 6. Test Rail

Four fuel tanks were fabricated using a 1/4-inch aluminum plate welded at the seams. The entire top portion of the fuel tank and the front opening contained removable covers, which were sealed using a fuel-resistant (high-temperature) gasket material. The top portion of the fuel tank had a vented fill cap. The weight of the fuel tank and other components are presented in table 3. The interior dimensions of the fuel tank were 2′ wide, 7′ long, and 1′ high, and the fuel tank had a fuel capacity of approximately 104 gallons. The weight of the test article varied based on the fuel level and type and is presented in table 4.

Table 3. Test Component Weights

Description	Weight (lb)
Empty fuel tank	280
Pusher sled	100
Zuni rocket (unburned)	82
Spacer plates total	47
Brake pads	10
Brake sled and calipers	181
Protective shroud	24
Total weight	724

Table 4. Total Assembly Weight Based on Fill Level and Fuel Type

Fill Level and Fuel Type	Fuel Weight (lb)	Total Weight (lb)
100% full (water)	875	1599
100% full (JP-8)	733	1457
84% full (water)	735	1459

A single, 5-inch-diameter Zuni rocket was chosen to accelerate the fuel tank in the test series. The Zuni rocket was selected based on the length limitations of the track, the payload size, and the velocities needed for this particular test. The design criterion required that the payload be accelerated to a peak velocity of approximately 180 to 220 fps without using more than 400 ft of track.

The braking system consisted of two spring-applied braking calipers from Kobelt Manufacturing Co., Ltd. attached to an aluminum sled (figure 7). An aluminum brake shroud (figure 8) was used to protect the braking system from excessive heat due to burning JP-8 fuel. The calipers were held open under 120 psi of air pressure. The pressurized air system consisted of the calipers, a piece of polyvinyl chloride (PVC) pipe that extended off the side of the brake sled, a fill nozzle, an on/off valve, and plumbing connecting the PVC pipe (figure 9). When the PVC pipe collided with a stationary pole located 225 ft down the rail (figure 10), the PVC pipe broke, releasing the pressure and allowing the calipers to clamp onto the rail.

Figure 7. Braking System

Figure 8. Aluminum Brake Shroud

Figure 9. The PVC Pipe and Braking System

Figure 10. Pole Used to Activate Brakes and Rupture the Fuel Tank

The fuel tank rupture system components are shown in figure 11. A 5-inch-diameter aluminum plate was used to cap the opening in the front face of the fuel tank. A 7-inch-diameter piece of aluminum foil tape was used to seal the plate to the fuel tank; this allowed for consistent and clean openings. A long bolt was fastened to the plate's center and was attached to a piece of steel pipe. The steel pipe was connected to a steel bracket on the corner of the fuel tank with a wooden dowel rod. Upon impact with the activation pole (figure 10), the arm would break the dowel rod and pivot outward, resulting in a 5-inch opening in the front face of the fuel tank.

Figure 11. Fuel Tank Rupture System Located on the Front of the Fuel Tank

An onboard data acquisition system (DAS) was used to record the internal pressures throughout the test (figure 12). Once triggered, the DAS recorded data at 10,000 Hz for 20 seconds. Three pressure transducers were threaded through the front face of the fuel tank and connected to the DAS. Successfully capturing pressure data proved to be a difficult task due to the nature of the test and the sensitivity of the equipment used. The majority of pressure data recorded during the fire tests was lost due to excessive heat, even after attempting to insulate the wires and DAS (figure 13). However, data captured during the water tests provided sufficient information to assess the performance of the LD foam. Temperature data were also recorded; however, fuel impinging upon the thermocouples prevented accurate temperature readings from being recorded.

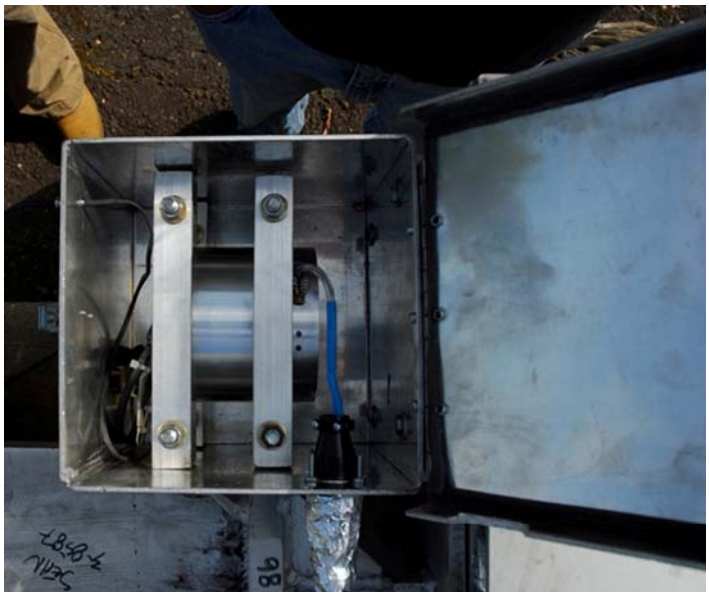

Figure 12. Onboard DAS, Protective Compartment, and Wiring

Figure 13. High-Temperature-Resistant Insulation Covering the DAS and Wiring

A series of cameras were positioned at different locations along the rail to capture the various stages of the test (figure 14). The leading face of the sled setup was positioned at the 25-foot location on the rail. All the cameras were initiated by a trigger box linked to fiber-optic break lines. Five cameras were used in the down-range setup and one camera was positioned up range to provide safe viewing of the rocket initiation. A Phantom high-speed video camera recording at 500 frames per second was positioned at the 250-foot mark with a relative angle of 90° to the rail. This camera was used to capture the initiation of the brake calipers and the rupturing of the fuel tank. A second Phantom high-speed video camera was positioned at the 600-foot mark with a relative angle of 150° to the rail. This camera was used to capture the dispersion of fuel and fireball that ensued from the fuel tank. A standard video camera, recording at 30 frames per second, was positioned in a 25-foot-high tower at the 1200-foot mark with a relative angle of 135° to the rail. The tower camera was used to capture the initiation, fireball, and pool fire that

occurred once the fuel tank stopped. An additional high-speed camera was used with a system called the Flight Follower. The system controls a parabolic mirror to follow a predetermined velocity profile, allowing the camera to capture movement along an extended range. However, because of the variability in the tests velocity profiles, the system failed to be useful for this evaluation. An attempt was made to capture the fireball using an onboard camera mounted to the brake sled. However, the camera and data were lost due to excessive heat.

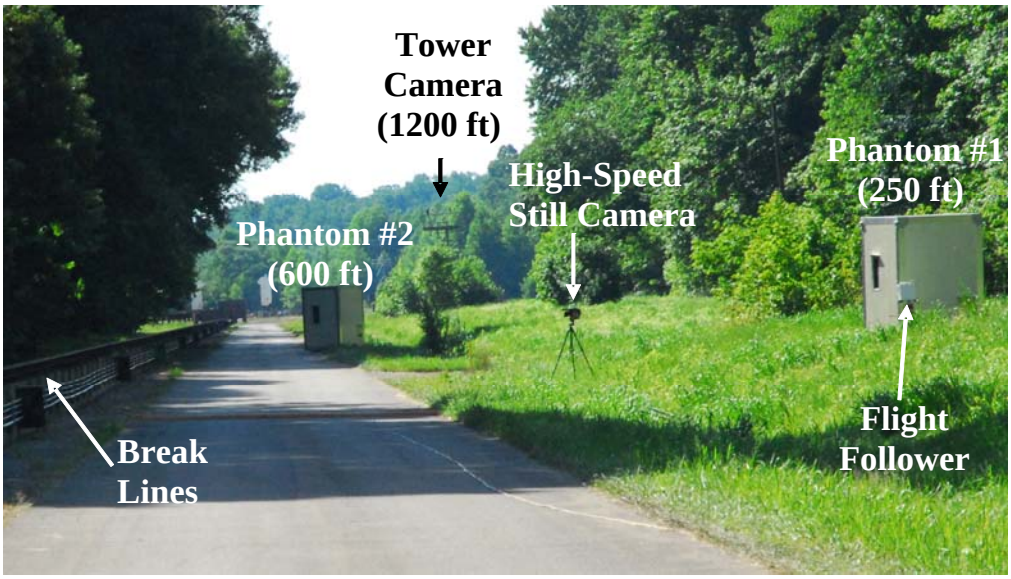

Figure 14. Down-Range Photography Setup

The position and velocity were captured using a 7.5-watt Weibel Doppler radar recording at 10,000 Hz (figure 15). The radar was set up 2200 ft down range from the starting point of the rocket sled. The radar was initiated 10 seconds prior to rocket initiation and recorded for 40 seconds.

Figure 15. Doppler Radar Head

4. TESTS.

All tests were conducted at the Ballistic Rail Facility, Aberdeen Proving Grounds, Edgewood, Maryland. Velocity and position measurements were acquired using radar, and the radar data was used to calculate acceleration data. The desired maximum velocity of the fuel tank was 180 to 220 fps, and the desired maximum deceleration of the fuel tank was 1.5 ±0.5 g. The desired stopping distance after the brakes were applied was approximately 500 ft. The front of the fuel tank was located at the starting location of the test (with the exception of the first and second test), approximately 2200 ft from the end of the rail (down range).

4.1 PHASE I.

4.1.1 Objective.

The objective of this phase was to

- characterize the performance of the propulsion/rail system under expected load conditions.
- determine wind resistance and friction coefficients necessary for the development of a braking system.

4.1.2 Test Setup.

The empty fuel tank was filled with water and sealed. The fuel tank and rocket-driven pusher sled were located at the start of the test rail (figure 16). The test was videotaped using three fixed video cameras focused on the initial, final, and the entire length of the test rail. The last 10 ft of the rail was recorded using high-speed cinematography to capture the final velocity of the fuel tank.

Figure 16. Shot No. 1 Setup

4.1.3 Results.

The maximum velocity for shot No. 1 was 231 ft/s at 237 ft and 1.77 seconds. The last recorded velocity was 164 ft/s at 2076 ft. The fuel tank left the end of the rail at the 2200-ft mark (figure 17) at an estimated velocity of 159 fps. The maximum calculated acceleration was 4.9 g's at 0.13 ft and 0.01 second. The maximum deceleration due to friction of the sled/rail and air resistance was 0.44 g at approximately 364 ft and 2.3 seconds, and the natural deceleration was 0.2 g. The velocity and acceleration data are presented as a function of sled position in figures 18 and 19, respectively. Evaluation of the radar data indicated that rocket burnout occurred just prior to the 225-ft mark. Thus, the 225-ft mark is the location that was used in future tests to activate the braking system and rupture the fuel tank.

Figure 17. Fuel Tank Leaving Rail

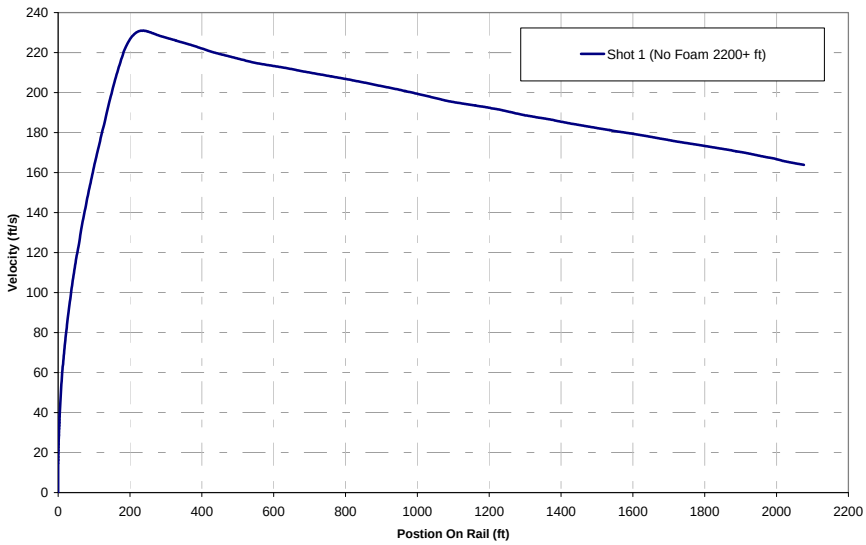

Figure 18. Shot No.1—Velocity vs Position

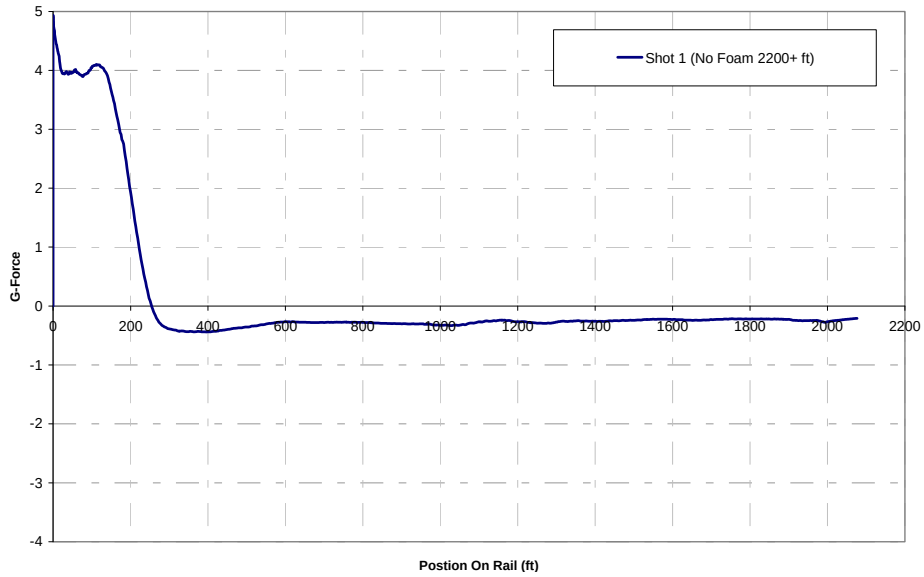

Figure 19. Shot No. 1—Acceleration vs Position

4.1.4 Technical Analysis.

A review of the video and radar data disclosed that

- the maximum velocity of the fuel tank (231 fps) exceeded the desired range (180 to 220 fps).
- a maximum deceleration of the fuel tank (0.44 g) was far below the desired range of 1.5 ±0.5 g's, and the fuel tank left the track at the end of 2200 ft.
- an external braking system was needed.
- the natural deceleration of the fuel tank was 0.2 g.
- a down-range distance of 225 ft from the start would be used as the location to initiate the automatic brake and rupture the fuel tank.

4.2 PHASE II.

4.2.1 Objectives.

The objectives for Phase II were to

- test and evaluate the automatic braking and fuel tank rupture systems.
- select the appropriate brakes for conducting the remaining test phases by evaluating two types of brake pad materials.

- identify the optimal placement for the ignition mechanism by visually mapping the dispersion of the surrogate fuel.

4.2.2 Test Setup.

The preshot setup for shot Nos. 2 and 3 is shown in figure 20. The fuel tank was filled with water and a braking system was installed. Ceramic brake pads were used for shot No. 2, and carbon metallic brake pads were used for shot No. 3. In shot No. 3, the fuel tank was instrumented with an onboard DAS, pressure transducers, and an accelerometer.

Figure 20. Shot Nos. 2 and 3 Setup

Automatic braking and fuel tank-rupturing systems were located at the 225-foot mark. The activation of both devices was captured over a 10-foot section of the rail using high-speed cinematography. The test was videotaped using three fixed video cameras focused on the burnout, final, and overall sections of the rail. The dispersion of the fuel was captured with high-speed cameras.

4.2.3 Test Results.

Shot No. 2 was completed on 20 December 2006. The maximum velocity was 188 ft/s at 181 ft and 1.7 seconds. The maximum acceleration was 3.8 g's at 95 ft and 1.2 seconds. The maximum deceleration was 0.92 g at 603 ft and 4.1 seconds, and the average deceleration after the brakes were applied was 0.27 g. Figure 21 shows shot No. 2 postrupture with water escaping from the fuel tank, and figure 22 shows the posttest fuel tank at rest.

Figure 21. Shot No. 2, Postrupture (dispersion of water)

Figure 22. Shot No. 2, Postrupture at Rest

Shot No. 3 was completed on 3 May 2007. The maximum velocity was 180 ft/s at 190 ft and 1.77 seconds. The maximum acceleration was 4 g's at 121 ft and 1.36 seconds. The maximum deceleration was 1.35 g's at 299 ft and 2.39 seconds and the average deceleration was 0.35 g. Figure 23 shows the fuel tank immediately after rupture. Figure 24 shows the fuel tank after traveling down the rail postrupture with water escaping from the front of the fuel tank, and figure 25 shows the posttest fuel tank at rest. The velocity and acceleration data are presented as a function of sled position in figures 26 and 27.

Figure 23. Shot No. 3, Immediately After Rupture

Figure 24. Shot No. 3, Postrupture (dispersion of water)

Figure 25. Shot No. 3, Postrupture at Rest

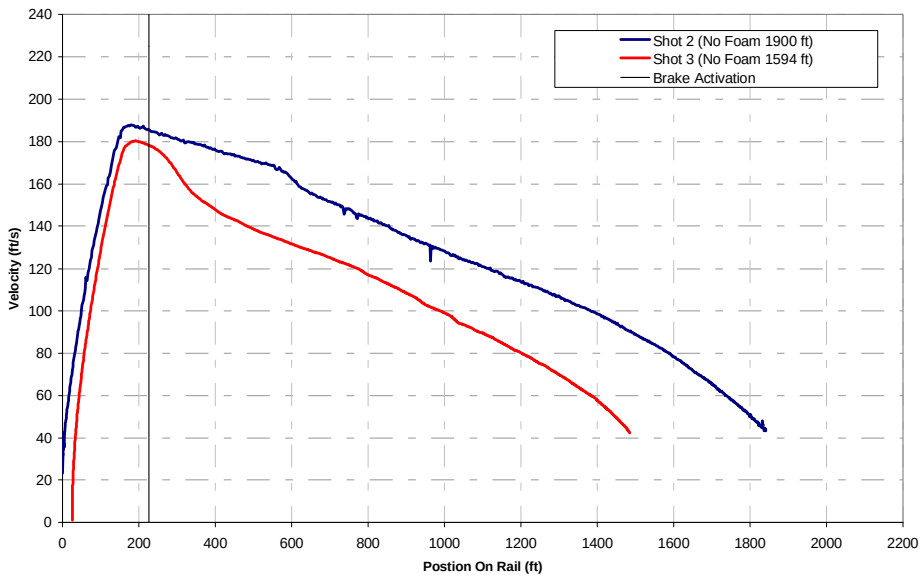

Figure 26. Shot Nos. 2 and 3—Velocity vs Position

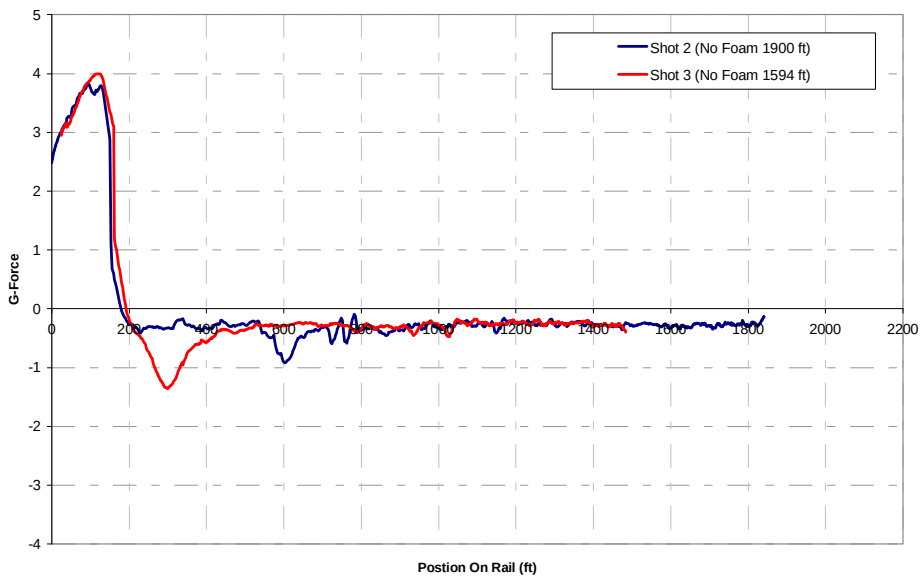

Figure 27. Shot Nos. 2 and 3—Acceleration vs Position

Detailed analysis of both tests showed that they had comparable initial velocity profiles prior to brake activation; however, the fuel tank for shot No. 3 stopped 306 ft earlier than shot No. 2 (figure 26). From the acceleration plot (figure 27), it is evident that the brake pads for shot No. 2 were ineffective after 400 ft, as the plot converges toward natural deceleration (0.27 g) after this point. This was due to brake pad failure from the excessive heat generated by the brake pads contacting the rail. The carbon metallic brakes used in shot No. 3 showed a great improvement over the ceramic brake pads used in shot No. 2 with regard to maximum deceleration and overall stopping distance.

4.2.4 Technical Analysis.

For shot No. 2, the maximum velocity of 188 fps met the test requirement of 180 to 220 fps. The maximum deceleration criterion of 1.5 ±0.5 g's was not met (0.92 g maximum and 0.27 g average). The ceramic brake pad used in shot No. 2 failed to decelerate the fuel tank as required.

For shot No. 3, the maximum velocity of 180 fps met the test requirement of 180 to 220 fps. The maximum deceleration criterion of 1.5 ±0.5 g's was met (1.35 g's maximum and 0.35 g average). The carbon metallic brake pad used in shot No. 3 failed to decelerate the fuel tank in the required distance.

However, the carbon metallic brake pad was the best pad material and formula available for this application and therefore was used for the remaining tests.

Subsequently, it was learned that successive shots imbedded pad material in the rail and greatly improved the braking ability, thus reducing the stopping distance.

4.3 PHASE III.

4.3.1 Objectives.

The objectives for Phase III were to

- evaluate the flow of fuel from the fuel tank with and without LD foam.
- measure the front inner wall pressures with and without LD foam.
- determine the dispersion dynamics of the water.

4.3.2 Test Setup.

In shots 4 through 8, the fuel tanks were configured as follows:

- Shot No. 4 was filled with water.
- Shot No. 5 was loaded with LD foam and then filled with water.
- Shot No. 6 was loaded with LD foam and then filled with water.
- Shot No. 7 was filled with water.
- Shot No. 8 was filled with water.

The preshot setup for shot Nos. 4 through 7, including instrumentation of the fuel tank, is shown in figure 28. The instrumentation was initialized and the rocket fired. Upon rocket burnout, mechanical braking was applied, and the fuel tank was ruptured. The activation of both devices was captured over a 10-foot section of the rail using high-speed cinematography. The fuel tank was fitted with an onboard DAS, pressure transducers, and an accelerometer. The test was videotaped using three fixed video cameras focused on the burnout, final, and entire length of the rail. The dispersion of the water was captured with high-speed cameras.

Figure 28. Shot No. 4 Pretest, Instrumented With Pressure Gauges

4.3.3 Test Results.

Shot No. 4 was completed on 3 May 2007. The maximum velocity was 174 ft/s at 184 ft and 1.79 seconds. The maximum acceleration was 3.6 g's at 102 ft and 1.26 seconds. The maximum deceleration was 1.52 g's at 314 ft and 2.57 seconds, and the average deceleration was 0.4 g. Figure 29 shows the postrupture fuel tank traveling down the rail with water escaping from the fuel tank. Figure 30 shows the posttest fuel tank at rest.

Figure 29. Shot No. 4, Postrupture (dispersion of water)

Figure 30. Shot No. 4, Postrupture at Rest

Shot No. 5 was completed on 7 May 2007. The maximum velocity was 195 ft/s at 203 ft and 1.78 seconds. The maximum acceleration was 4.22 g's at 132 ft and 1.39 seconds. The maximum deceleration was 1.58 g's at 310 ft and 2.35 seconds, and the average deceleration was 0.2 g. Figures 31 and 32 show the LD foam in the fuel tank. Figure 33 shows the fuel tank postrupture, traveling down the rail with water escaping from the fuel tank.

Figure 31. Shot No. 5, Fuel Tank With LD Foam—Notched Cutout for Pressure Gauges

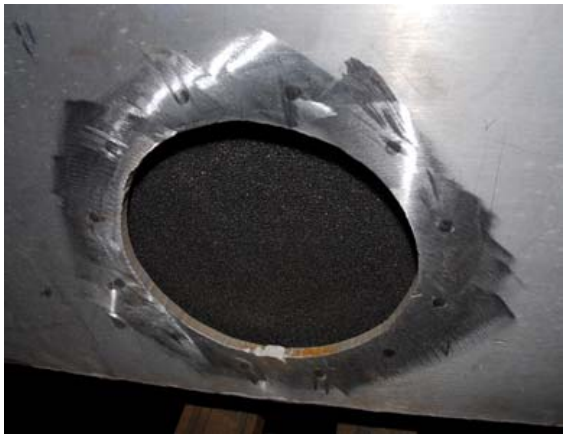

Figure 32. Shot No. 5, Front View of the LD Foam in the Fuel Tank

Figure 33. Shot No. 5, Postrupture (dispersion of water)

Shot No. 6 was completed on 11 September 2007. The maximum velocity was 184 ft/s at 202 ft and 1.81 seconds. The maximum acceleration was 3.9 g's at 124 ft and 1.36 seconds. The maximum deceleration was 1.40 g's at 314 ft and 2.44 seconds, and the average deceleration was 0.6 g. Figure 34 shows the fuel tank postrupture, traveling down the rail with water escaping from the fuel tank. A preshot setup of the LD foam in the fuel tank is shown in figure 35, and the deformation of the LD foam posttest is shown in figure 36.

Figure 34. Shot No. 6, Postrupture (dispersion of water)

Figure 35. Shot No. 6, Fuel Tank With two Pieces of LD Foam

Figure 36. Shot No. 6, 3/4″ Deformation of LD Foam due to Inertia

Shot No. 7 was completed on 12 September 2007. The maximum velocity was 183 ft/s at 203 ft and 1.86 seconds. The maximum acceleration was 3.9 g's at 129 ft and 1.43 seconds. The maximum deceleration was 1.63 g's at 314 ft and 2.49 seconds, and the average deceleration was 0.6 g. Figure 37 shows the postrupture fuel tank traveling down the rail with water escaping from the fuel tank. Figure 38 shows the posttest fuel tank at rest.

Figure 37. Shot No. 7, Postrupture (dispersion of water)

Figure 38. Shot No. 7, Posttest at Rest

Shot No. 8 was completed on 13 September 2007. The maximum velocity was 190 ft/s at 204 ft and 1.8 seconds. The maximum acceleration was 3.7 g's at 80 ft and 1.01 seconds. The maximum deceleration was 1.65 g's at 347 ft and 2.61 seconds, and the average deceleration was 0.5 g. Figure 39 shows the postrupture fuel tank traveling down the rail with water escaping from the fuel tank.

Figure 39. Shot No. 8, Postrupture (dispersion of water)

For Phase III, velocity as a function of position is shown in figure 40, and acceleration as a function of position is shown in figure 41.

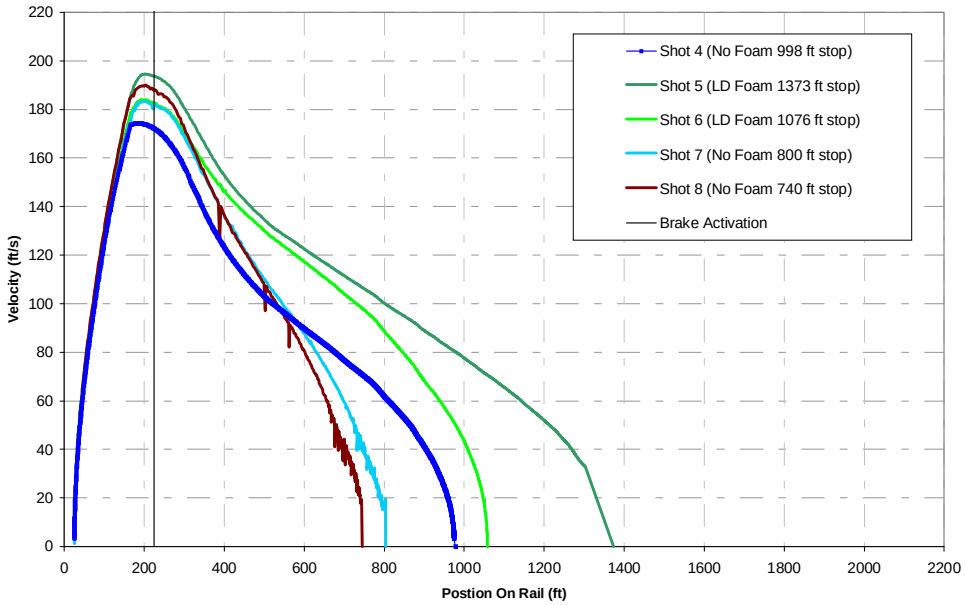

Figure 40. Shot Nos. 4 to 8, Velocity vs Position

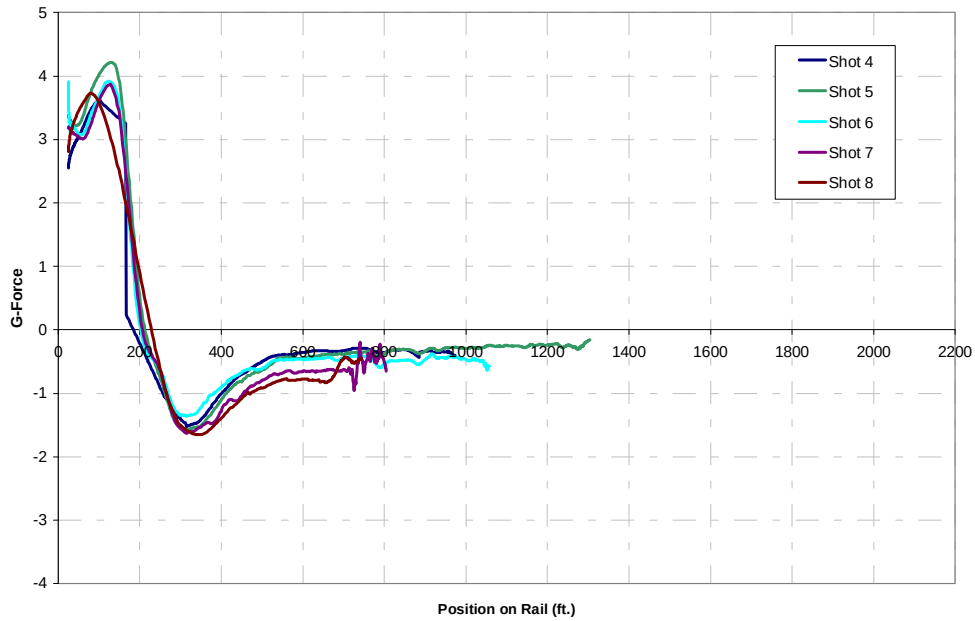

Figure 41. Shot Nos. 4 to 8, Acceleration vs Position

Shot Nos. 5 and 6 with LD foam traveled further and had a lower average maximum deceleration than shot Nos. 4, 7, and 8 without LD foam. This led to the conclusion that the LD foam prevented the fuel from escaping, as explained. Assuming the clamping force of the calipers was the same between tests, then according to the following equation, the mass of the fuel tanks with LD foam must be larger than those without LD foam to generate the above results.

$$F_{friction} = \mu_k F_N \tag{1}$$

where $F_{friction}$ is the force due to kinetic friction, μ_k is the coefficient of kinetic friction, and F_N is the normal force. Since the weight of the LD foam is negligible, the data show evidence that the LD foam must have been successful in mitigating the flow of fuel through the simulated rupture. This observation was supported by visual inspection of the fuel tank at the end of each test. The fuel tank with the LD foam retained approximately 50% to 66% of the liquid while the fuel tank without the LD foam was empty.

With or without LD foam, the stopping distances decreased for each respective test with the increasing number of shots. Therefore, using equation 1, the coefficient of kinetic friction increased as braking material became embedded in the rail.

4.3.4 Technical Analysis.

For shot No. 4, the maximum velocity of 174 fps did not meet the test requirement of 180 to 220 fps. The maximum deceleration criterion of 1.5 ±0.5 g's was met (1.52 g's maximum and 0.4 g average).

For shot No. 5, the maximum velocity of 203 fps met the test requirement of 180 to 220 fps. The maximum deceleration criterion of 1.5 ±0.5 g's was met (1.58 g's maximum and 0.2 g average).

For shot No. 6, the maximum velocity of 184 fps met the test requirement of 180 to 220 fps. The maximum deceleration criterion of 1.5 ±0.5 g's was met (1.40 g's maximum and 0.6 g average).

For shot No. 7, the maximum velocity of 183 fps met the test requirement of 180 to 220 fps. The maximum deceleration criterion of 1.5 ±0.5 g's was met (1.63 g's maximum and 0.6 g average).

For shot No. 8, the maximum velocity of 190 met the test requirement of 180 to 220 fps. The maximum deceleration criterion of 1.5 ±0.5 g's was met (1.65 g's maximum and 0.5 g average).

As the braking system applied a constant force to the calipers, the decreased deceleration levels (increased stopping distances) of the LD foam tests indicate that the LD foam prevented the loss of water from the fuel tank. The results are consistent with the posttest observations of the fuel tank.

With or without LD foam, the stopping distances decreased for each respective test with the increasing number of shots. Therefore, the coefficient of kinetic friction increased as braking material became embedded in the rail.

4.4 PHASE IV.

4.4.1 Objectives.

The objectives for Phase IV were to

- evaluate the performance of standard road flares as a fuel ignition source.
- use a surrogate fuel (water) level that more closely approximated the payload incurred by Jet JP-8 fuel.
- fabricate and install a braking system protective shroud.
- evaluate an external ignition system for fuel.

Note: JP-8 has an approximate specific gravity of 0.84; therefore, the fuel tank was filled with water to the 84% fill level.

4.4.2 Test Setup.

To protect the braking system from the fire and heat during the fuel test, a protective shroud was fabricated and installed (figure 42). Road flares were mounted to the fuel tank (figure 43) and evaluated to determine their ability to ignite leaking fuel in the upcoming fuel tests. The fuel tank was filled with water to the 84% fill level. The flares were initiated with electric matches before rocket initiation. Upon rocket burnout, mechanical braking was applied and the fuel tank was ruptured. The activation of both the braking and fuel tank-rupturing devices was captured over a 10-foot section of the rail using high-speed cinematography. The fuel tank was fitted with an onboard DAS, pressure transducers, and an accelerometer. The test was videotaped using three fixed video cameras focused on the burnout, final, and entire length of the rail. The dispersion of the fuel was recorded with high-speed cameras.

Figure 42. Shot No. 9, Protective Shroud Surrounding Braking System

Figure 43. Shot No. 9, Road Flares Added to Ignite Fuel

4.4.3 Test Results.

Shot No. 9 was completed on 8 August 2007. The maximum velocity was 190 fps at 207 ft and 1.82 seconds. The maximum acceleration was 3.9 g's at 129 ft and 1.38 seconds. The maximum deceleration was 1.38 g's at 309 ft and 2.38 seconds, and the average deceleration was 0.7 g.

Velocity as a function of position is shown in figure 44, and acceleration as a function of position is shown in figure 45.

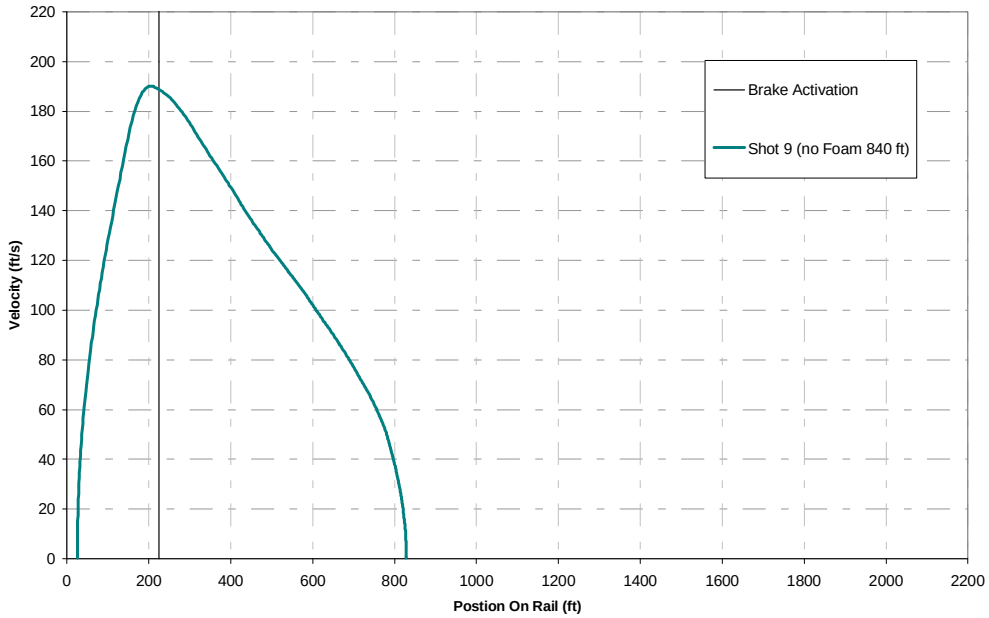

Figure 44. Shot No. 9—Velocity vs Position

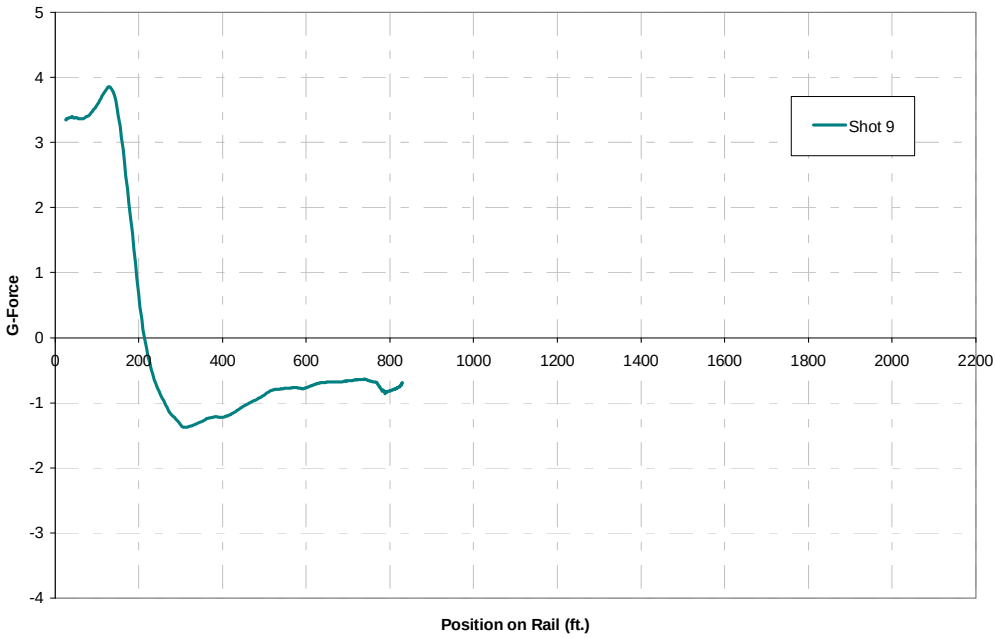

Figure 45. Shot No. 9—Acceleration vs Position

4.4.4 Technical Analysis.

A review of the video and radar data disclosed that

- the maximum velocity of 190 fps met the test requirement of 180 to 220 fps. The maximum deceleration criterion of 1.5 ±0.5 g's was met (1.38 g's maximum and 0.7 g average).

- the roadside flares used in shot No. 9 failed to remain lit when water contacted them. Magnesium flares were used for subsequent tests, and two additional locations were added for a higher probability of ignition.

4.5 PHASE V.

4.5.1 Objectives.

The objectives for Phase V were to

- conduct two redundant JP-8 fuel tests without LD foam.

- evaluate the dispersion of fuel and the fire threat level.

- perform a qualitative assessment on the performance of the LD foam by analyzing the high-speed cinematography.

- determine the severity of the fire event, such as the burning duration, fuel distribution, fire size, and fireball occurrence.

4.5.2 Test Setup.

The setup procedures for shot Nos. 10 and 11 were identical. The magnesium flares used to ignite the escaping fuel were mounted on the fuel tank, as shown in figure 46. The instrumentation lines were insulated to protect them against fire and heat (figure 47). The fuel tank was filled with JP-8 fuel, the fuel tank was sealed, the systems were initialized, and the rocket was fired. Upon rocket burnout, mechanical braking was applied and the fuel tank was ruptured. The activation of both the braking and fuel tank-rupturing devices was captured over a 10-foot section of the rail using high-speed cinematography. The fuel tank was fitted with an onboard DAS, pressure transducers, and an accelerometer. The test was videotaped using three fixed video cameras focused on the burnout, final, and entire length of the rail. The dispersion of the fuel was recorded with high-speed cameras. Upon completion, the burning fuel was extinguished by the fire department, and the site was cleaned.

Figure 46. Shot No. 10, Magnesium Flares Used to Ignite Fuel

Figure 47. Shot No. 10, Insulated Instrumentation Lines

4.5.3 Test Results.

Shot No. 10 was completed on 5 September 2007. The maximum velocity was 219 fps at 229 ft and 1.8 seconds. The maximum acceleration was 4.4 g's at 140 ft and 1.4 seconds. The maximum deceleration was 1.57 g's at 354 ft and 2.4 seconds, and the average deceleration was 0.7 g. Figures 48 and 49 show the fuel tank traveling down the rail surrounded by a fireball, and figure 50 shows the fuel tank at rest and the fire extinguished. Approximately 7 minutes after the fuel tank came to rest, it was inspected; only a small amount of fuel remained in the fuel tank.

Figure 48. Shot No. 10, Postrupture

Figure 49. Shot No. 10, Postrupture—Close-Up

Figure 50. Shot No. 10, Postrupture at Rest

Shot No. 11 was completed on 17 October 2007. The maximum velocity was 184 fps at 196 ft and 1.68 seconds. The maximum acceleration was 4.26 g's at 0 ft and 0 seconds (time of ignition). The maximum deceleration was 1.58 g's at 306 ft and 2.3 seconds, and the average deceleration was 0.9 g. The resulting postignition fireball, as the fuel tank was traveling down the rail, is shown in figure 51. The damage to the fuel tank and the braking system caused by the fire are shown in figures 52 and 53. Velocity as a function of position is shown in figure 54, and acceleration as a function of position is shown in figure 55. Pressure data for shot No. 11 are provided in figure 56. Approximately 7 minutes after the fuel tank came to rest, it was inspected; only a small amount of fuel remained in the fuel tank.

Figure 51. Shot No. 11, Postrupture

Figure 52. Shot No. 11, Postrupture at Rest

Figure 53. Shot No. 11, Postrupture at Rest—Damaged Shroud

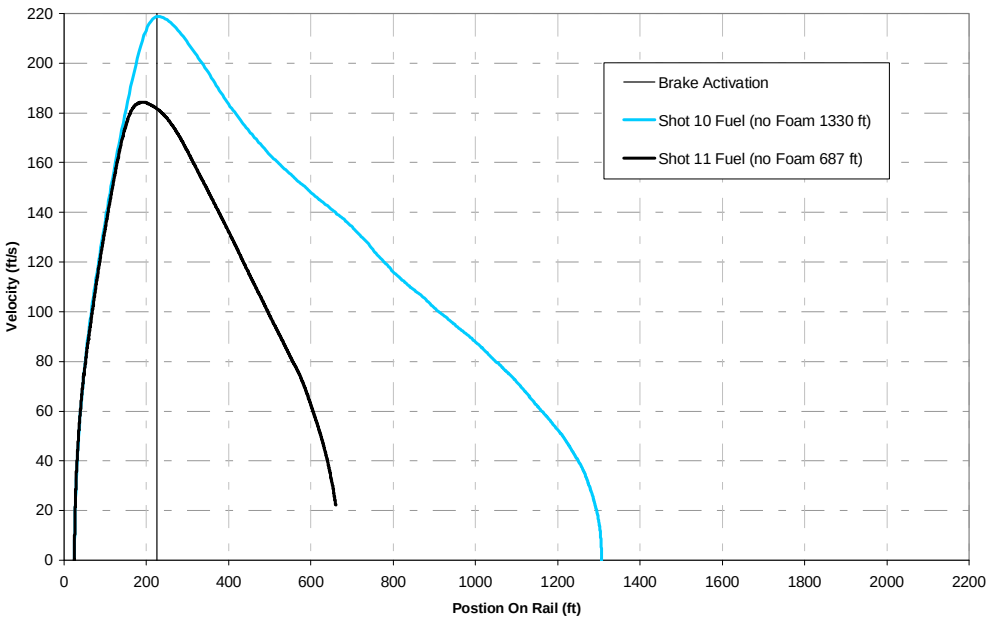

Figure 54. Shot No. 11—Velocity vs Position

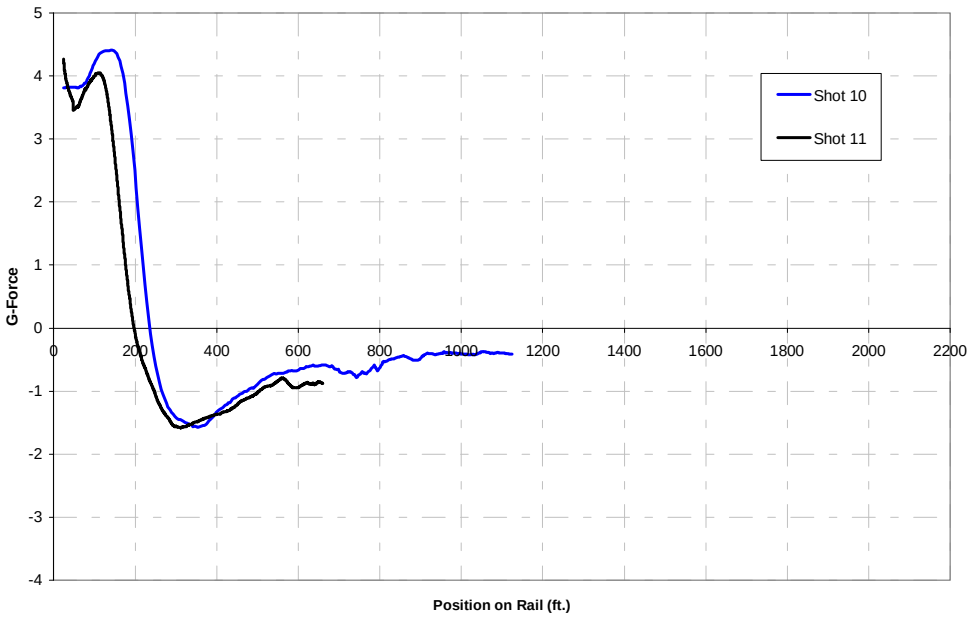

Figure 55. Shot No. 11—Acceleration vs Position

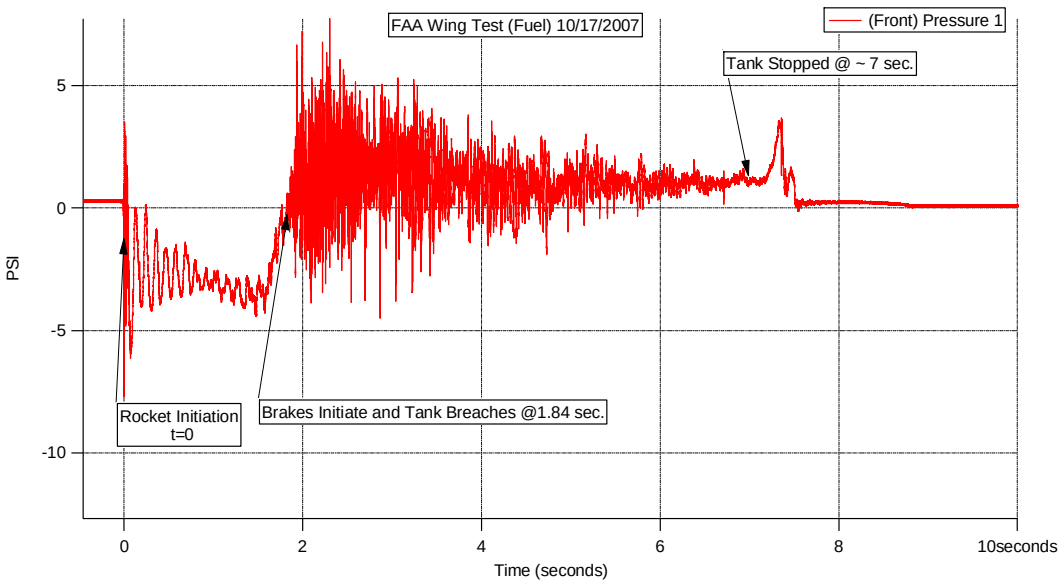

Figure 56. Shot No. 11—Pressure Data

4.5.4 Technical Analysis.

For shot No.10, the maximum velocity of 219 fps met the test requirement of 180 to 220 fps. The maximum deceleration criterion of 1.5 ±0.5 g's was met (1.57 g's maximum and 0.7 g average).

For shot No.11, the maximum velocity of 184 fps met the test requirement of 180 to 220 fps. The maximum deceleration criterion of 1.5 ±0.5 g's was met (1.58 g's maximum and 0.9 g average).

- The magnesium flares used in shot Nos. 10 and 11 successfully ignited the fuel.
- Posttest inspection, after the fuel tank came to rest, revealed that only a small amount of fuel remained in the fuel tank.

4.6 PHASE VI.

4.6.1 Objectives.

The objectives for Phase V were to

- conduct two redundant JP-8 fuel tests with LD foam.
- evaluate the mitigation abilities of the LD foam on dispersion of the fuel and the fire threat level.
- perform a qualitative assessment on the performance of the LD foam by analyzing the high-speed cinematography.

- determine the severity of the fire event, such as the burning duration, fuel distribution, fire size, and fireball occurrence.

4.6.2 Test Setup.

The setup procedures for shot Nos. 12 and 13 were identical to shot Nos. 10 and 11, except the fuel tank contained LD foam. Figure 57 shows the LD foam in the fuel tank before the test. Preshot setups for shot Nos. 12 and 13 are shown in figures 58 and 59, respectively. The fuel tank was filled with JP-8 fuel, the fuel tank was sealed, the systems were initialized, and the rocket was fired. Upon rocket burnout, mechanical braking was applied and the fuel tank was ruptured. The activation of both the braking and fuel tank-rupturing devices was captured over a 10-foot section of the rail using high-speed cinematography. The fuel tank was fitted with an onboard DAS, pressure transducers, and an accelerometer. The test was videotaped using three fixed video cameras focused on the burnout, final, and entire section of the rail. The dispersion of the fuel was recorded with high-speed cameras. Upon completion, the burning fuel was extinguished by the fire department, and the site was cleaned.

Figure 57. Shot No. 12, Fuel Tank With two Pieces of LD Foam

Figure 58. Shot No. 12, Pretest

Figure 59. Shot No. 13, Fuel Tank With two Pieces of LD Foam

4.6.3 Test Results.

Shot No. 12 was completed on 8 November 2007. The maximum velocity was 167 fps, which was lower than the acceptable velocity. The maximum acceleration of 3.9 g's was consistent with the other tests. However, the maximum deceleration of 3.08 g's was significantly greater than the pervious tests. In addition, the acceleration profile suggests that the maximum deceleration was even greater than the peak recorded value. The fuel tank stopped in 463 ft, which is significantly shorter than the previous tests. Therefore, the test was repeated (shot No. 13) to gather comparable data to the previous fuel shots without LD foam. Figure 60 shows the fireball after fuel tank rupture, and figure 61 shows the posttest damage. Approximately 7 minutes after the fuel tank came to rest, it was inspected; approximately 50% to 66% of the fuel remained in the fuel tank.

Figure 60. Shot No. 12, Postrupture Fuel Test With LD Foam

Figure 61. Shot No. 12, Postrupture at Rest

Shot No. 13 was completed on 18 December 2007. The maximum velocity was 187 fps, which is comparable to previous tests. The maximum acceleration of 4.2 g's was consistent with the other tests. The maximum deceleration of 1.95 g's was also comparable to previous tests. However, unlike previous tests, the brakes on the fuel tank did not burn out, and the fuel tank did not return to natural deceleration (0.27 g) but maintained a constant deceleration of about 1.5 g's (average 1.6 g's). Therefore, this test served as an accurate worst-case scenario in comparison to the previous tests without LD foam.

The resulting fireball and damage was similar to Shot No. 12 (figures 60 and 61). The damage to the LD foam after the shot is shown in figure 62. Velocity as a function of position is presented in figure 63, and acceleration as a function of position is shown in figure 64. Approximately 7 minutes after the fuel tank came to rest, it was inspected; approximately 50% to 66% of the fuel remained in the fuel tank.

Figure 62. Shot No. 13, Front View of LD Foam Removed From Fuel Tank

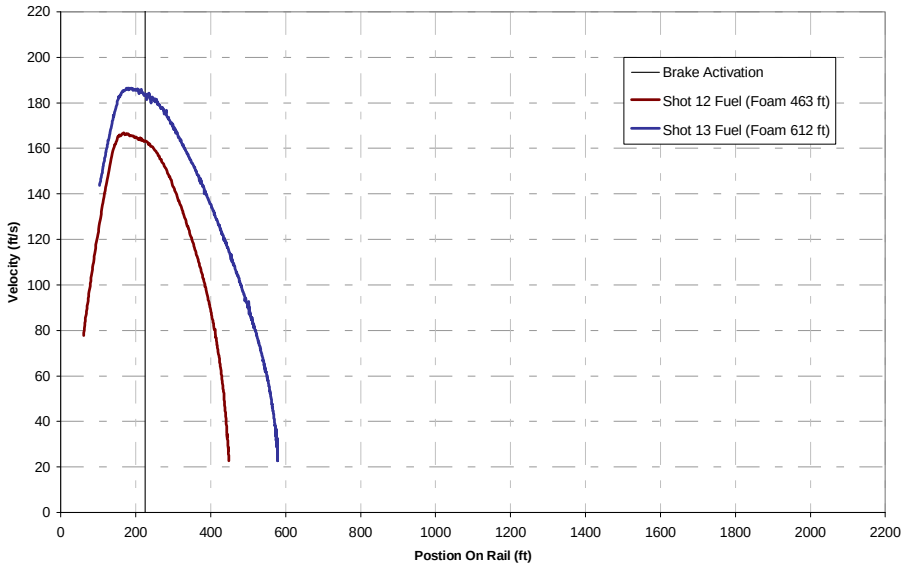

Figure 63. Shot Nos. 12 and 13—Velocity vs Position

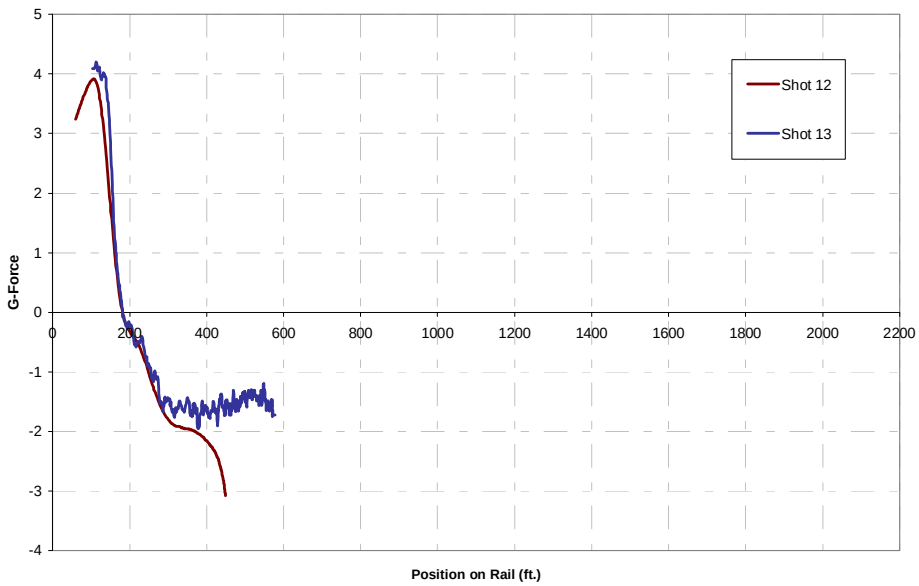

Figure 64. Shot Nos. 12 and 13—Acceleration vs Position

4.6.4 Technical Analysis.

For shot No. 12, the maximum velocity of 167 fps did not meet the test requirement of 180 to 220 fps. The maximum deceleration criterion of 1.5 ±0.5 g's was exceeded (3.08 g's maximum and 0.7 g average).

For shot No.13, the maximum velocity of 187 fps met the test requirement of 180 to 220 fps. The maximum deceleration criterion of 1.5 ±0.5 g's was met (1.95 g's maximum and 1.55 g's average).

The LD foam acted as a plug allowing only 50% to 66% of the fuel to leak from the fuel tank.

4.7 PHASE VII.

4.7.1 Objectives.

The objectives of Phase VII were to compare the results of the previous tests to

- evaluate the effect LD foam has on the internal pressures observed within the fuel tank and throughout the entirety of the test.
- evaluate the effect LD foam has on the dispersion of the fuel from the fuel tank upon rupture and deceleration.
- evaluate the LD foam's effect on the ensued fireball from the fuel tank upon rupture and deceleration.
- evaluate the LD foam's effect on the pool fire that ensued once the fuel tank came to rest.

4.7.2 Test Results.

A summary of the test matrix and the results are provided in appendix A, and the results are described below.

- Internal Pressure—Shot Nos. 4 and 5 were used to compare the no LD foam versus LD foam internal pressures, respectively. The fuel tanks experienced similar g-forces during deceleration; however, shot No. 5 underwent a higher initial acceleration (figure 65). The location of the pressure gage used for the comparison was mid-depth on the front face of the fuel tank. The internal pressures shown in figure 66 show a strong reduction in the pressure experienced with the addition of the LD foam. Figures 66 and 67 show that the oscillation in the pressure due to sloshing was greatly reduced with the addition of the LD foam. The negative pressure readings were due to the gauge facing away from the direction of travel. The noise during the deceleration portion of the data was attributed to the vibrations of the brakes against the rail. Peak pressure levels were decreased by approximately 50% despite higher acceleration levels achieved in the test using LD foam (4.2 g's versus 3.6 g's).
- Dispersion of fuel—Shot Nos. 4 and 5 were also compared to determine the ability of the LD foam to reduce the amount of fuel that escapes from the fuel tank upon deceleration. Figures 68 and 69 show each fuel tank experiencing deceleration of -1.25 g's and moving at 95 mph (140 fps). Surrogate fuel was used to illustrate dispersion to reduce the environmental impact. The images clearly illustrate the reduction of fuel escaping the fuel tank with the LD foam in place.
- Fireball—Shot Nos. 11 and 13 were chosen to compare the ensuing fireball in the no LD foam versus LD foam cases. The velocity for both shot Nos. 11 (no LD foam) and 13 (LD foam) were almost identical with differences occurring near the end of the tests

(figure 70). Both fuel tanks experienced similar g-forces during acceleration; however, shot No. 13 underwent a larger and more constant deceleration (figure 71). The velocity and acceleration data were used to validate that similar forces were experienced for both test cases.

- High-speed video was compared for shot Nos. 11 and 13 allowing a visual assessment to be made as to the magnitude of the fireball generated for each case (figure 72). The high-speed images show a strong discrepancy between the LD foam and no LD foam cases. The size and intensity of the fireball was greatly reduced with the LD foam in place. To aid in the visual comparison, figures 73 and 74 show a series of tower images illustrating the development of the fireball as the fuel tank moved down the rail. The series images are presented at one image per second and represent the same position and time for shot Nos. 11 (no LD foam) and 13 (LD foam) in figures 73 and 74, respectively.

- Pool fire—Shot Nos. 11 and 13 were also used to compare the magnitude of the pool fire in the no LD foam versus LD foam cases. A series of images illustrating the development of the pool fire from the stopped fuel tank were used for visual comparison. The series of images are presented at one image per 5 seconds, beginning 15 seconds after rocket initiation. The images represent the same position and time for shot Nos. 11 (LD foam) and 13 (no LD foam) in figures 75 and 76. Examination of the video demonstrated that the LD foam decreased the growth of the pool fire by reducing the rate at which the fuel leaked out of the fuel tank. The size and intensity of the pool fire was greatly reduced with the LD foam in place. To explain this further, it is necessary to note that leaking fuel fed from the adjacent wing sections would flow freely from the no LD foam crash. This would feed the external pool fire. On the other hand, the LD foam would slow the flow of fuel from the adjacent sections, thereby reducing the fire threat.

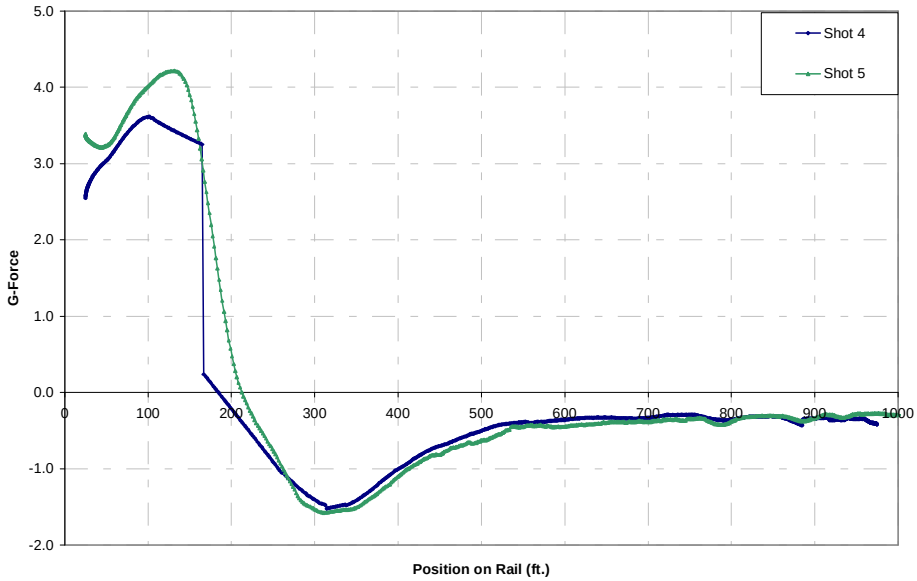

Figure 65. Shot Nos. 4 and 5—Acceleration vs Position on Rail

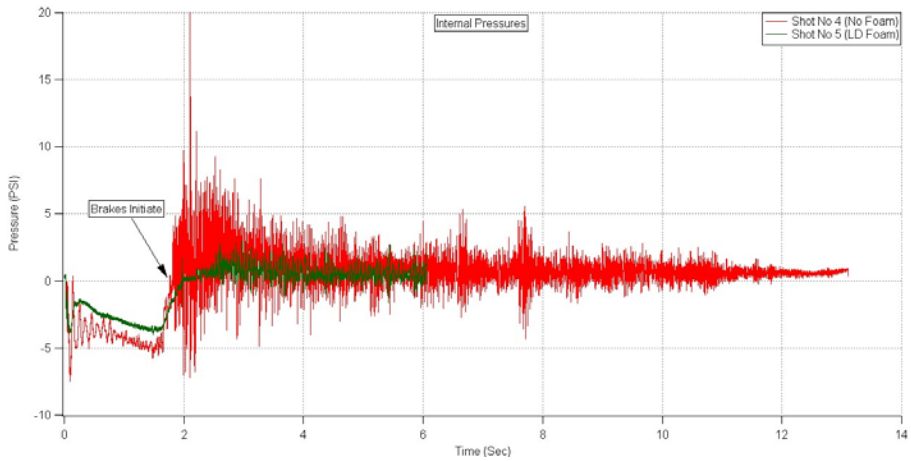

Figure 66. Shot Nos. 4 and 5, Internal Pressures

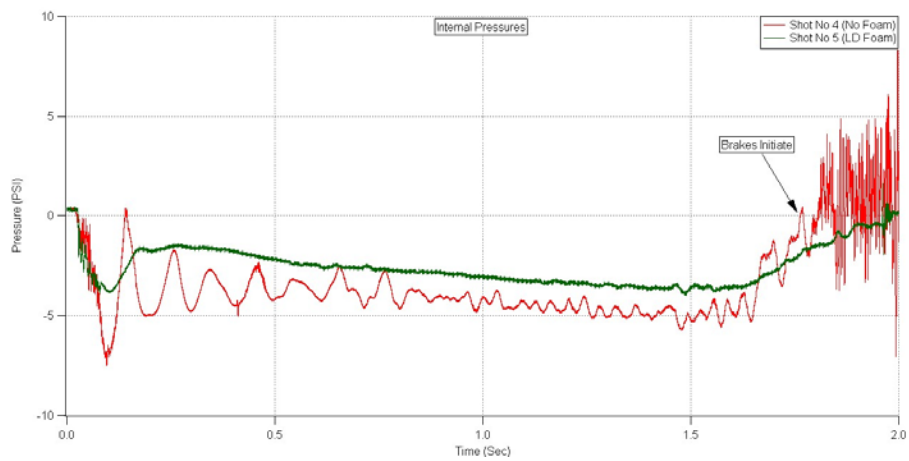

Figure 67. Shot Nos. 4 and 5, Internal Pressures—Close-Up

Figure 68. Shot No. 4, Dispersion of Water While Decelerating (-1.25 g), no LD Foam

Figure 69. Shot No. 5, Dispersion of Water While Decelerating (-1.25 g), With LD Foam

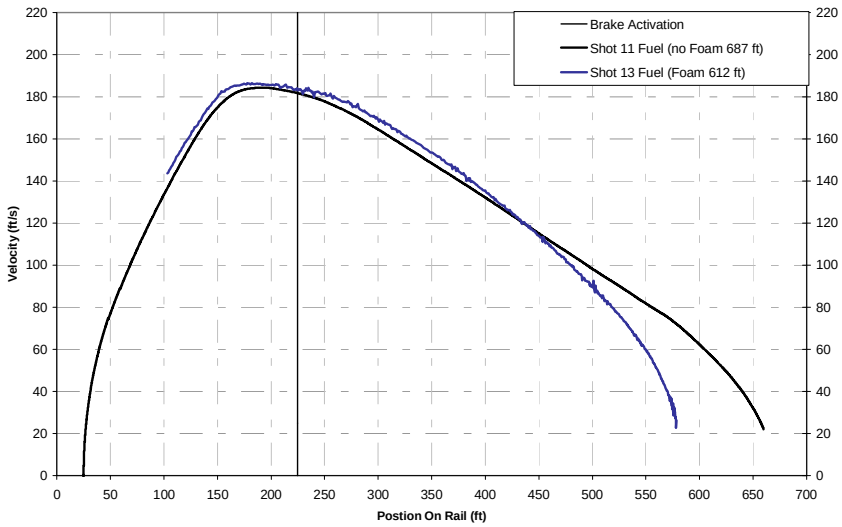

Figure 70. Shot Nos. 11 and 13—Velocity vs Position

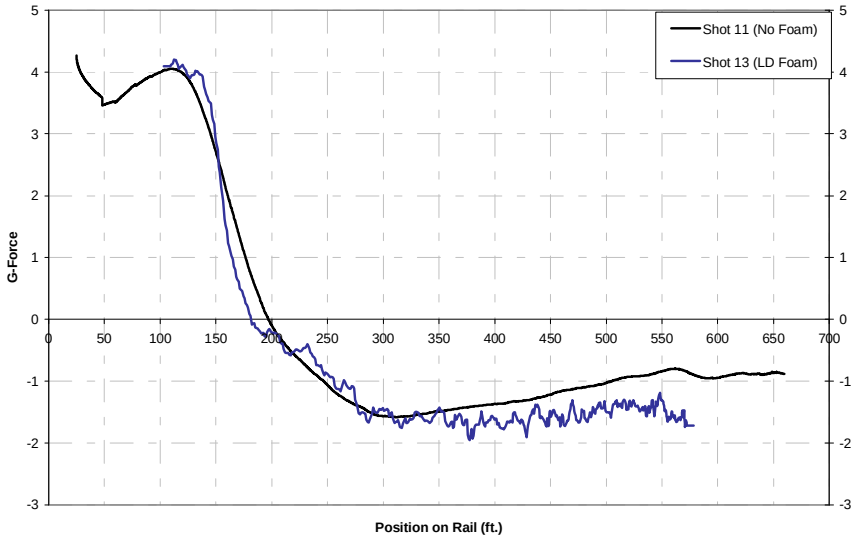

Figure 71. Shot Nos. 11 and 13—Acceleration vs Position

(a) Shot No. 11, Without LD Foam

(b) Shot No. 13, With LD Foam

Figure 72. Shot Nos. 11 and 13, Comparison of Burning JP-8 Fireball

Figure 73. Shot No. 11 (no LD Foam), 1-Second Series of Tower Images of the Fireball

Figure 74. Shot No. 13 (LD Foam), 1-Second Series of Tower Images of the Fireball

Figure 75. Shot No. 11 (no LD Foam), 5-Second Series of Tower Images of the Fireball

Figure 76. Shot No. 13 (LD Foam), 5-Second Series of Tower Images of the Fireball

5. CONCLUSIONS.

A series of simulated impact tests were conducted to determine the effectiveness of a low-density (LD) reticulated foam insert designed to be placed inside a simulated fuel cell to reduce or stop the flow of fuel under dynamic inertial loading in a simulated crash. The test article was a simulated fuel tank representing a section of a large commercial transport airplane. The fuel tank was mounted to a sled filled with JP-8 fuel or a surrogate (water) and propelled down a test track at approximately 130 mph (190 ft/s). The fuel tank represented one section of a large aircraft that was ruptured by simulating a leading-edge impact, resulting in a 5-inch opening in the front spar.

Tests showed that the LD foam was successful in reducing the fuel tank's internal pressure against the front face of the fuel tank. This would correspond to reduce fuel sloshing within the fuel tank. The LD foam acted as a plug and reduced the size of the fireball and water/fuel dispersion during the deceleration phase. Posttest inspection of the fuel tank, approximately 7 minutes after the fuel tank came to rest, showed that (1) without LD foam, most of the liquid leaked out of the fuel tank and (2) with LD foam, approximately 50% to 66% of the liquid remained in the fuel tank, and the leakage rate was very low. Given that fuel in the adjacent sections would have flowed to, and out of, the ruptured opening, the size and magnitude of a resulting postcrash, fuel-fed pool fire would have been greater for a fuel tank without LD foam.

Table A-1. Test Matrix and Results

Phase	Shot No.	LD Foam	Fuel Type	% Full	Braked	Ruptured	Fire	Weight (lb)	Distance Traveled (ft)	Velocity Maximum (ft/s)	Acceleration Maximum (g)	Deceleration Maximum (g)	Deceleration Constant (g)	Data	Date Completed
I	1	No	Water	100	No	No	No	1599	200+	231	4.93	0.44	0.2	v,x	24-Oct-05
II	2	No	Water	100	Yes	Yes	No	1599	1900	188	3.94	0.92	0.27	v,x	20-Dec-06
	3	No	Water	100	Yes	Yes	No	1599	1594	180	4.00	1.35	0.35	P,T,v,a,x	2-May-07
III	4	No	Water	100	Yes	Yes	No	1599	996	184	3.61	1.52	0.4	P,T,v,a,x	3-May-07
	5	Yes	Water	100	Yes	Yes	No	1599	1373	203	4.22	1.58	0.2	P,T,v,a,x	7-May-07
	6	Yes	Water	100	Yes	Yes	No	1599	1076	184	3.91	1.40	0.6	P,T,v,a,x	11-Jul-07
	7	No	Water	100	Yes	Yes	No	1599	800	183	3.87	1.63	0.6	P,T,v,a,x	12-Jul-07
	8	No	Water	100	Yes	Yes	No	1599	740	190	3.73	1.65	0.5	P,T,v,a,x	13-Jul-07
IV	9	No	Water	84	Yes	Yes	No	1459	840	190	3.86	1.38	0.7	P,T,v,a,x	8-Aug-07
V	10	No	JP-8	100	Yes	Yes	Yes	1457	1330	219	4.41	1.57	0.7	P,T,v,a,x	5-Sep-07
	11	No	JP-8	100	Yes	Yes	Yes	1457	678	184	4.26	1.58	0.9	P,T,v,a,x	17-Oct-07
VI	12	Yes	JP-8	100	Yes	Yes	Yes	1457	463	167	3.92	3.08	-	P,T,v,a,x	8-Nov-07
	13	Yes	JP-8	100	Yes	Yes	Yes	1457	612	187	4.20	1.95	1.55	v,a,x	18-Dec-07

x = Distance traveled
a = Acceleration
v = Velocity
P = Pressure
T = Temperature

Phase I—Demonstration
Phase II—External braking system evaluation
Phase III—Surrogate fuel (water) performance evaluation
Phase IV—Flare and water level evaluation
Phase V—Fuel performance evaluation
Phase VI—LD foam performance evaluation